ORIGINAL ARTICLE

Cancer Science WILEY

TIP60 is required for tumorigenesis in non-small cell lung cancer

Daisuke Shibahara[1] | Naoki Akanuma[1,2] | Ikei S. Kobayashi[1] | Eunyoung Heo[1,3] | Mariko Ando[1] | Masanori Fujii[1] | Feng Jiang[4] | P. Nicholas Prin[1] | Gilbert Pan[1] | Kwok-Kin Wong[5] | Daniel B. Costa[1] | Deepak Bararia[6] | Daniel G. Tenen[6,7] | Hideo Watanabe[4] | Susumu S. Kobayashi[1,6,8]

[1]Department of Medicine, Beth Israel Deaconess Medical Center, Harvard Medical School, Boston, Massachusetts, USA

[2]Department of Pathology, University of California San Francisco, San Francisco, California, USA

[3]Department of Internal Medicine, SMG-SNU Boramae Medical Center, Seoul, South Korea

[4]Division of Pulmonary, Critical Care and Sleep Medicine, Department of Medicine, Department of Genetics and Genomic Sciences, Tisch Cancer Institute, Icahn School of Medicine at Mount Sinai, New York, New York, USA

[5]Perlmutter Cancer Center, NYU Langone Medical Center, New York, New York, USA

[6]Harvard Stem Cell Institute, Harvard Medical School, Boston, Massachusetts, USA

[7]Cancer Science Institute of Singapore, National University of Singapore, Singapore, Singapore

[8]Division of Translational Genomics, Exploratory Oncology Research and Clinical Trial Center, National Cancer Center, Kashiwa, Japan

Correspondence
Susumu S. Kobayashi, Department of Medicine, Beth Israel Deaconess Medical Center, Harvard Medical School, 330 Brookline Avenue, E/CLS-0409, Boston, MA 02215, USA.
Email: skobayas@bidmc.harvard.edu

Funding information
National Cancer Institute, Grant/Award Number: CA197697, CA218707 and CA240257

Abstract

Histone modifications play crucial roles in transcriptional activation, and aberrant epigenetic changes are associated with oncogenesis. Lysine (K) acetyltransferases 5 (TIP60, also known as KAT5) is reportedly implicated in cancer development and maintenance, although its function in lung cancer remains controversial. Here we demonstrate that TIP60 knockdown in non-small cell lung cancer cell lines decreased tumor cell growth, migration, and invasion. Furthermore, analysis of a mouse lung cancer model with lung-specific conditional *Tip60* knockout revealed suppressed tumor formation relative to controls, but no apparent effects on normal lung homeostasis. RNA-seq and ChIP-seq analyses of inducible TIP60 knockdown H1975 cells relative to controls revealed transglutaminase enzyme (TGM5) as downstream of TIP60. Investigation of a connectivity map database identified several candidate compounds that decrease TIP60 mRNA, one that suppressed tumor growth in cell culture and *in vivo*. In addition, TH1834, a TIP60 acetyltransferase inhibitor, showed

comparable antitumor effects in cell culture and *in vivo*. Taken together, suppression of TIP60 activity shows tumor-specific efficacy against lung cancer, with no overt effect on normal tissues. Our work suggests that targeting TIP60 could be a promising approach to treating lung cancer.

KEYWORDS
artemisinin, KAT5, lung cancer, TGM5, TIP60

1 | INTRODUCTION

Lung cancer is the leading cause of cancer-related deaths in the USA and worldwide. Despite the marked development of treatments such as targeted therapy or immunotherapy in the past two decades, more than 100,000 Americans died from lung cancer in 2021.[1] As most patients with advanced lung cancer develop acquired resistance to existing treatments, novel therapies for lung cancer are imperative. Histone modifications, including lysine acetylation, play crucial roles in transcriptional activation, transcript elongation, gene silencing, and epigenetic cellular memory, and aberrant epigenetic changes are associated with oncogenesis.[2] Among epigenetic modifiers, the aberrant activity of several lysine (K) acetyltransferases (KATs) is implicated in cancer development. KATs, which are subdivided based on the sequence of their catalytic domains, comprise three major subfamilies: (a) GCN5 and PCAF, (b) p300 and CBP, and (c) MYST (Moz, Ybf2/Sas3, Sas2, and TIP60). TIP60, also known as KAT5, is the founding member of the MYST family, whose members function in chromatin remodeling, gene regulation, dosage compensation, DNA damage repair, and tumorigenesis by acetylating histone or non-histone proteins.[3] TIP60 function in cancer development is complex. TIP60, as part of the multisubunit NuA4 complex, is recruited to target promoters by various transcription factors. Within the NuA4 complex, TIP60 acetylates the nucleosomal histones H2A and H4 and acts as a coactivator of transcriptional factors.[4] Conversely, TIP60 also functions in p53 activation, contributing to the induction of apoptosis[5-7] and is required for expression of KAI1, a tumor suppressor in prostate cancer.[8] Thus, TIP60 activity appears to be context dependent, and aberrant lysine acetyltransferase activity can either promote or suppress tumorigenesis in colon, breast, and prostate cancers.[8-11] Here, given that a function for TIP60 in lung cancer is also controversial, we investigated TIP60 function using *in vitro* cell culture and *in vivo* lung cancer models and searched for TIP60 effectors. We found that TIP60 serves as a coactivator to promote tumorigenesis in the context of lung cancer and that targeting TIP60 could serve as a treatment for lung cancer.

2 | MATERIALS AND METHODS

The materials and methods are described in Data S1.

2.1 | Results

2.2 | Low levels of TIP60 expression are required for tumorigenesis in lung cancer

First, we examined the TIP60 expression level in various human organs using GTEx datasets and found that TIP60 is ubiquitously expressed at various levels in multiple organ systems, including the lung (Figure 1A). We then investigated TIP60 expression in various NSCLC lines: three (H1975, HCC827, and PC9) that harbor activating *EGFR* mutations, three (H358, H460, and A549) that harbor *KRAS* mutations, one each that harbors *BRAF* mutations (H1395), the *EML4-ALK* fusion gene (H3122), and a *ROS1* fusion gene (HCC78), as well as BEAS-2B, an immortalized human bronchial epithelial cell line. Western blot analysis showed that all lines expressed four TIP60 splice variant isoforms at various TIP60 levels, although six out of nine NSCLC lines expressed lower levels of TIP60 than did BEAS-2B cells (Figure 1B). To confirm these findings in clinical samples, we analyzed the data from TCGA lung adenocarcinoma dataset. Comparative analysis revealed significantly lower TIP60 expression in lung adenocarcinoma relative to normal lung tissues (Figure 1C), suggesting that TIP60 serves as a tumor suppressor in lung cancers. To test this hypothesis, we selected H1975 and A549 (each harboring *EGFR* or *KRAS* mutations and both expressing lower TIP60) cells, and established the TIP60 overexpressing (OE) cells. Immunoblot analysis and qPCR confirmed TIP60 overexpression in H1975-OE cells and A549-OE cells (Figure 2A, and Figure S1A); however, contrary to our hypothesis, TIP60 OE did not decrease cell growth of either line (Figure 2B,C). Furthermore, TIP60 OE had no significant effect on migration and invasion in H1975 (Figure 2D,F) and A549 cells (Figure 2E,G). Different splice variant isoforms also had no significant effects on tumor growth (Figure S1B–F), suggesting that TIP60 does not function as a tumor suppressor in lung cancer.

Next, to investigate the effects of TIP60 silencing in cell culture, we tried to generate TIP60 knockout cells in H1975 using CRISPR-Cas9 but obtained no homozygous knockout cells (data not shown). Thus we generated H1975 or A549 cells that harbored DOX-inducible small hairpin RNA (shRNA) targeting TIP60. Doxycycline treatment of both lines specifically suppressed TIP60 expression at both mRNA (Figure S2A,B) and protein levels (Figure 3A,B) in two different shRNA clones of each (shTIP60-1 and shTIP60-2). We then
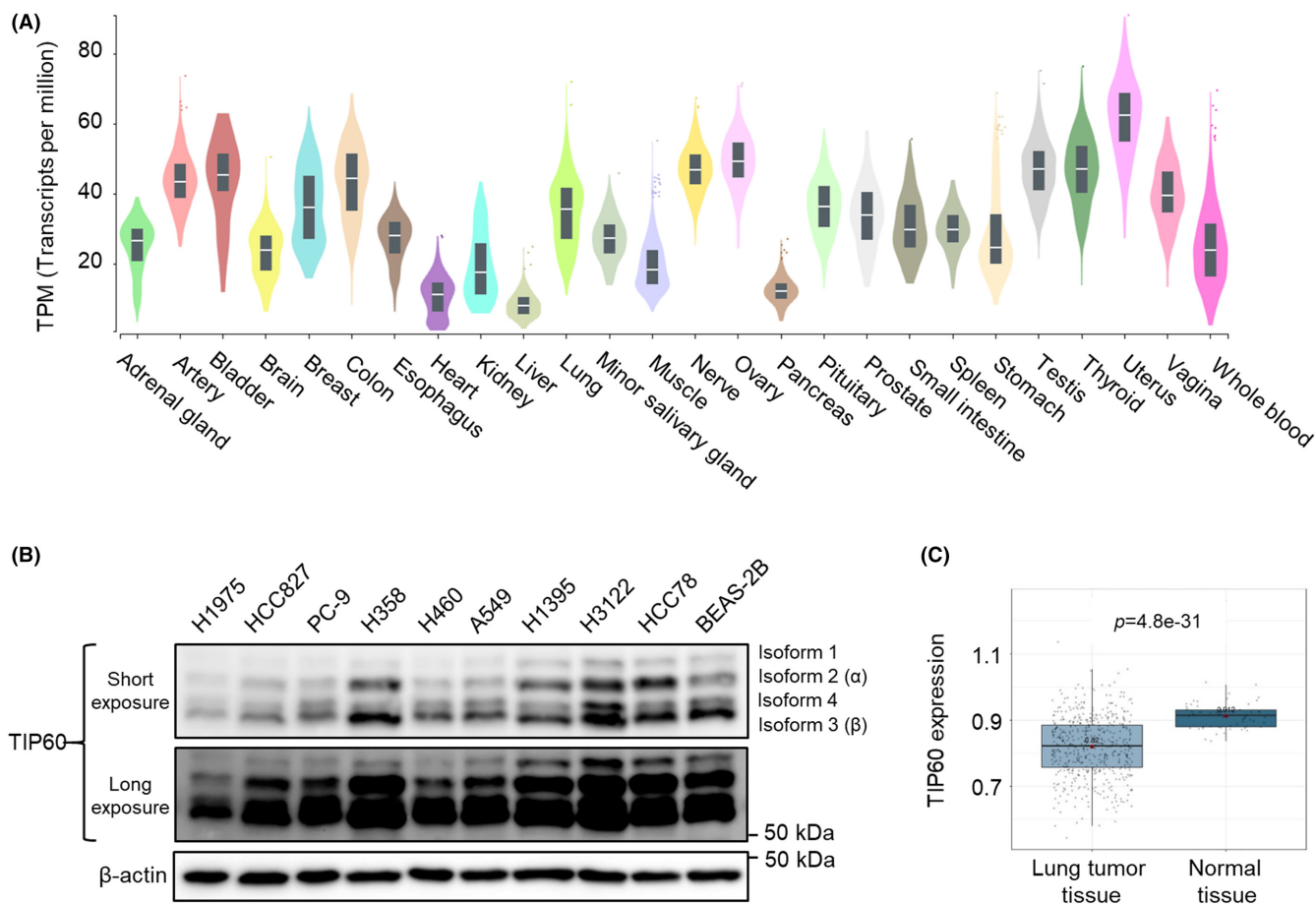
(A)

(B)

(C)

FIGURE 1 TIP60 is expressed at lower levels in lung cancer lines and clinical lung tumor tissues than in normal. (A) TIP60 expression in various human tissues in the GTEx dataset. Expression values are shown as transcripts per million (TPM) and presented as a violin plot for each tissue type. Violin plots are shown as median and 25th and 75th percentiles; points are displayed as outliers if they are above or below 1.5 times the interquartile range. (B) Immunoblot showing four TIP60 splice variant isoforms at varying levels in several lung cancer lines and in the immortalized normal alveolar cell line (BEAS-2B). Isoforms 2 and 3 are also known as the α form and β form, respectively. Immunoblot data are representative of three independent experiments. (C) Comparative analysis of TCGA adenocarcinoma dataset showing lower TIP60 expression in lung tumor ($n = 517$) than in normal lung tissues ($n = 59$). Boxes show medians with upper and lower quartiles, and whiskers represent minimum and maximum values. For comparative analysis, the p-value was calculated using the unpaired two-tailed Welch's t-test.

observed that, following DOX treatment and consequent *TIP60* suppression, H1975 and A549 cells (each harboring shTIP60-2) significantly decreased cell growth relative to controls not treated with DOX (Figure 3C,D). To assess migration activity in these lines, we performed a wound healing assay and found that TIP60 knockdown significantly decreased H1975 cell migration by day 1 (Figure 3E) and A549 cell migration by day 3 (Figure 3F). Furthermore, TIP60 knockdown significantly suppressed invasive activities of H1975 and A549 cells relative to controls not treated with DOX (Figure 3G,H). Analysis in both lines using corresponding shTIP60-1 clones showed comparable cell growth, migration, and invasion activities (Figure S2C–E). To confirm that enzymatic activity of TIP60 is required for tumorigenesis, constructs of wild-type (WT) TIP60, TIP60-G380A (inactive mutation, mut)[12,13] or an empty vector were transiently transfected into TIP60 knockdown cells (H1975 shTIP60-2 under DOX treatment). Immunoblot analysis confirmed continuous suppression of TIP60 with DOX treatment in empty transfected cells, and TIP60 overexpression in TIP60-WT, or TIP60-mut transfected

cells (Figure S3A). Wild-type TIP60 increased the acetylation of Histone H4 (Figure S3A), resulting in a significant increase in tumor cell growth, migration, and invasive activities, although TIP60 carrying the inactive mutation had no effect on acetyltransferase activity nor tumor growth (Figure S3A–D). Interestingly, the knockdown of TIP60 expression in BEAS-2B cells showed no effect on cell growth and migration activities (Figure S4A–C). Taken together, these results indicated that lung cancers showed relatively low TIP60 expression, which is essential for their survival, and that further suppressing TIP60 acetyltransferase activity antagonizes their tumorigenicity.

2.3 | *Tip60* knockout inhibits tumorigenesis in mouse lung cancer

To assess the effects of TIP60 silencing *in vivo*, we generated *Tip60* conditional knockout mice (*Tip60*$^{F/F}$)[14,15] (Figure S5A). To determine whether TIP60 contributed to normal lung homeostasis,
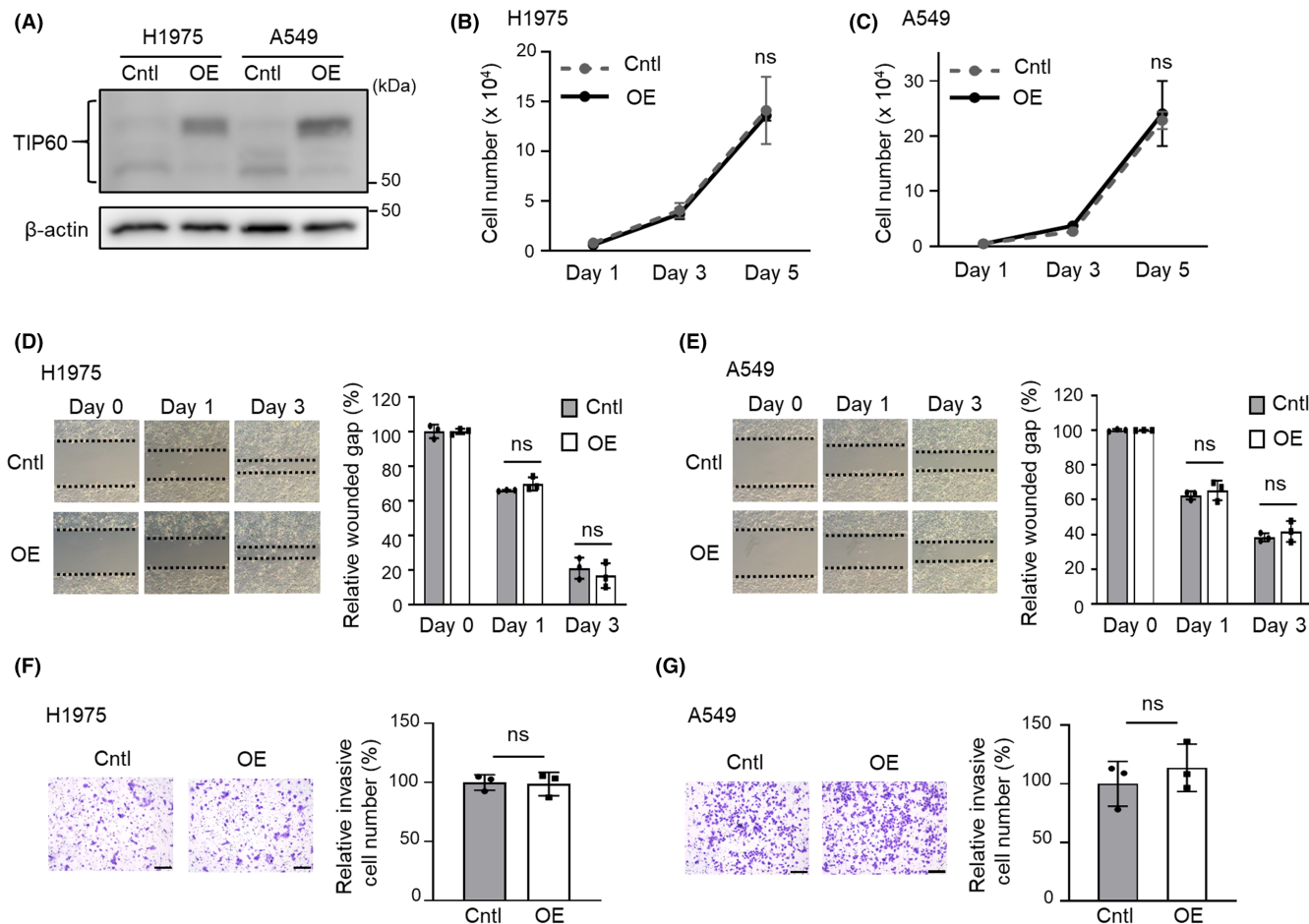
FIGURE 2 TIP60 overexpression does not alter tumor progression. (A) Immunoblot showing TIP60 overexpression efficiency in H1975 and A549 cells. Cntl; mock-transfected cells, OE; TIP60-overexpressing cells. Blots show representative images. (B, C) Cell growth assay in control or H1975 (B) and A549 (C)-OE cells. Data are the mean ± SD of triplicates from one experiment and are representative of three independent experiments. (D, E) Wound healing assay showing no significant difference in migration activities between TIP60 OE H1975 (D) and A549 (E) cells versus the corresponding control cells. Images of wounded cell monolayers are representative of three independent experiments. Data are the mean ± SD of triplicates from one experiment and are representative of three independent experiments. (F, G) Transwell invasion assay showing no significant difference in invasion activities between TIP60 OE H1975 (F) and A549 (G) cells versus corresponding control cells. Images of invasive cells are representative of two independent experiments. Data are the mean ± SD of three invasive cell number/field from one experiment and are representative of two independent experiments. Scale bars: 200 μm. The *p*-value was calculated using the unpaired two-tailed Welch's *t*-test. ns; not significant.

we started by generating *CCSP-rtTA/Cre/Tip60^{F/F}* mice, in which TIP60 is lost only in alveolar epithelial cells following DOX treatment. Once juvenile mice became 3–5 weeks of age, we treated them with DOX for 8–10 weeks. After 8–10 weeks of treatment, we isolated the lungs for histological analysis. That analysis revealed no significant histological differences in lung cells among *CCSP-rtTA/Cre/Tip60^{wt/wt}*, *CCSP-rtTA/Cre/Tip60^{F/wt}*, and *CCSP-rtTA/Cre/Tip60^{F/F}* genotype mice (Figure S5B). We then crossed lung-specific EGFR-L858R-T790M (*EGFR^{TL}*) transgenic mice (*TetOp-EGFR^{TL}/CCSP-rtTA*)—a mouse model of lung cancer[16]— with conditional *Tip60* knockout mice that had been crossed with tetracycline-inducible *Cre*-expressing mice (*TetOp-Cre/Tip60^{F/F}*) to generate *EGFR^{TL}/CCSP-rtTA/Cre/Tip60^{F/F}* mice (Figure S5A). We then performed PCR analysis to confirm proper recombination in *Tip60^{wt/wt}*, *Tip60^{F/wt}*, and *Tip60^{F/F}* mice as well as *EGFR* transgene

expression (Figure 4A). Significantly, lungs isolated from *EGFR^{TL}/CCSP-rtTA/Cre/Tip60^{F/F}* (IV) mice appeared similar to normal lungs (I) at 8–10 weeks after DOX treatment, while lungs isolated from *EGFR^{TL}/CCSP-rtTA/Cre/Tip60^{wt/wt}* (II) or *EGFR^{TL}/CCSP-rtTA/Cre/Tip60^{F/wt}* (III) mice exhibited tumors by 8 weeks after DOX treatment (Figure 4B). Moreover, lungs from *EGFR^{TL}/CCSP-rtTA/Cre/Tip60^{wt/wt}* (II) or *EGFR^{TL}/CCSP-rtTA/Cre/Tip60^{F/wt}* (III) mice were significantly heavier than lungs from *CCSP-rtTA/Cre/Tip60^{F/wt}* (I) mice, while lungs isolated from *EGFR^{TL}/CCSP-rtTA/Cre/Tip60^{F/F}* (IV) mice appeared similar to normal lungs (I) (Figure 4B,C). No significant difference was observed in lung appearance and weight between (II) and (III). Hematoxylin and eosin staining of lung tissue revealed that lungs isolated from *EGFR^{TL}/CCSP-rtTA/Cre/Tip60^{F/F}* (IV) mice did not show signs of overproliferation or tumor formation, whereas we observed tumor formation in lungs
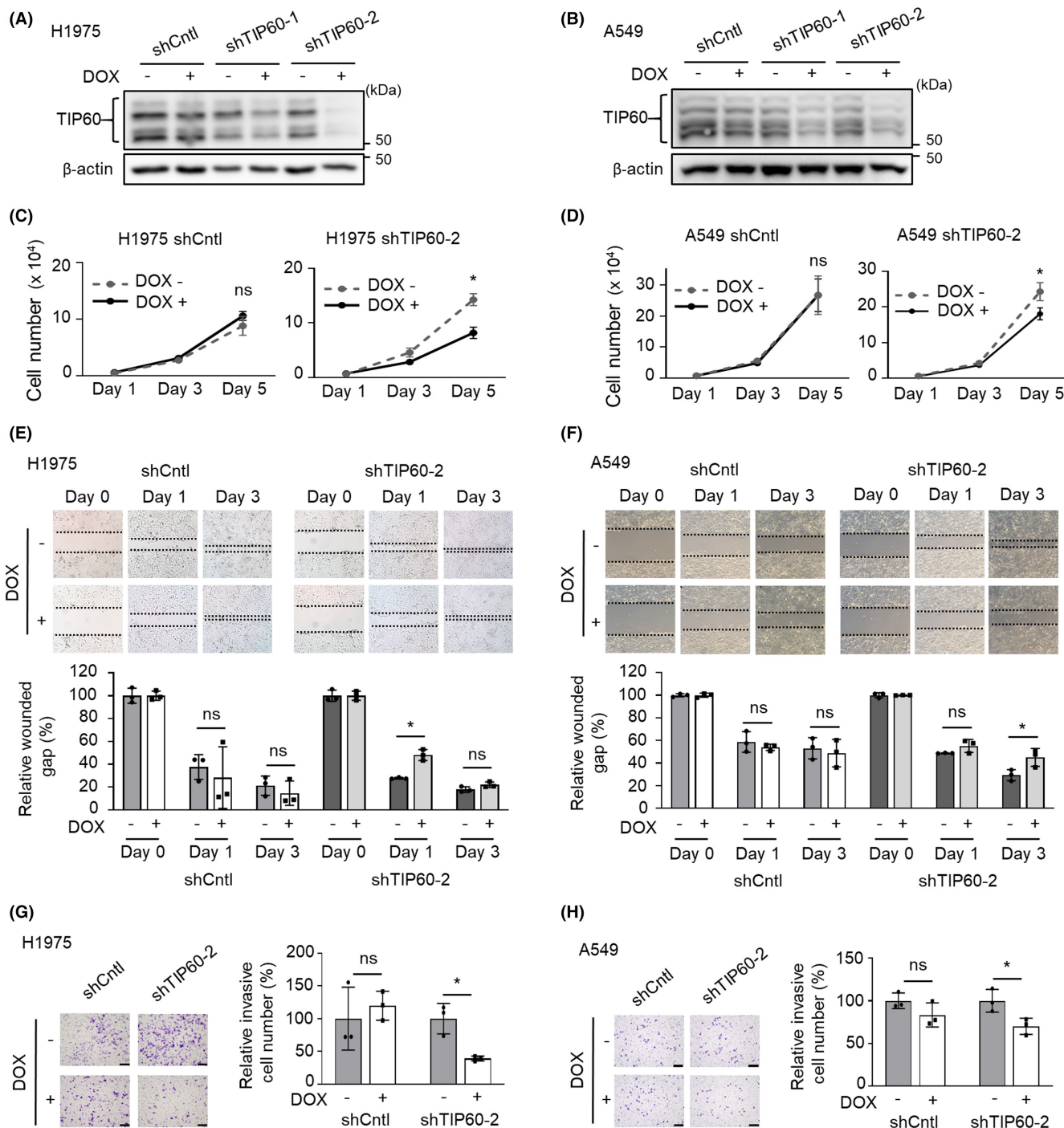
FIGURE 3 TIP60 knockdown inhibits tumor growth, migration, and invasion activities. (A, B) Immunoblot showing TIP60 knockdown efficiency in H1975 (A) or A549 (B) shTIP60-1 and shTIP60-2 cells. After 72h of doxycycline treatment (0.5 μg/mL), proteins were subjected to immunoblot. All blots show representative images. (C, D) TIP60 knockdown inhibits cell growth in H1975 (C) or A549 (D) shTIP60-2 cells. Cell numbers were determined on days 1, 3, and 5 after doxycycline (0.5 μg/mL) addition. Data are the mean±SD of triplicates from one experiment and are representative of three independent experiments. (E, F) H1975 (E) or A549 (F) shTIP60-2 cells show a decreased migration compared with the control cells. Wound gaps (day 0) were made after 24h of doxycycline treatment and overnight serum starvation. Images of wounded cell monolayers are representative of three independent experiments. Data are the mean±SD of triplicates from one experiment and are representative of three independent experiments. (G, H) Transwell invasion assay showing significant difference in invasion activities between H1975 (G) or A549 (H) shTIP60-2 cells versus the corresponding control cells. Images of invasive cells are representative of three independent experiments. Data are the mean±SD of three invasive cell number/field from one experiment and are representative of three independent experiments. Scale bars: 200 μm. The *p*-value was calculated using the unpaired two-tailed Welch's t-test. *$p < 0.05$. ns; not significant.
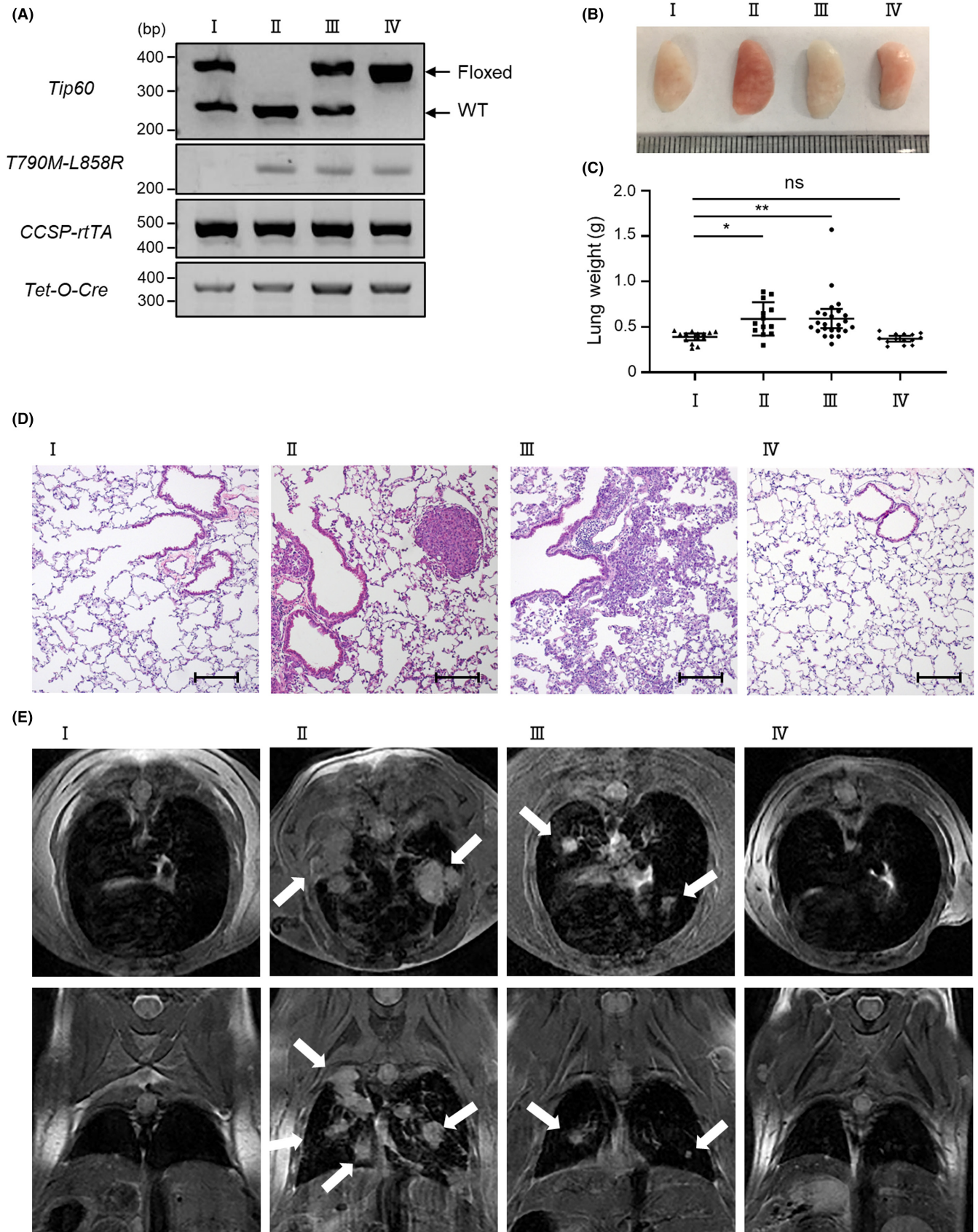
FIGURE 4 *Tip60* knockout lung cancer model mice show no tumor formation in the lung. (A) PCR of genomic DNA to confirm the genotypes of homozygous *Tip60* knockout (F/F), heterozygous *Tip60* knockout (F/wt), or wild-type (wt/wt) mice, as well as the EGFR transgene: I, *CCSP-rtTA/Cre/Tip60$^{F/wt}$*, II, *EGFR^{TL}/CCSP-rtTA/Cre/Tip60$^{wt/wt}$*, III, *EGFR^{TL}/CCSP-rtTA/Cre/Tip60$^{F/wt}$*, and IV, *EGFR^{TL}/CCSP-rtTA/Cre/Tip60$^{F/F}$*. (B, C) Appearance and weight of lungs in each mouse group: I ($n = 14$), II ($n = 13$), III ($n = 24$), IV ($n = 14$). Data are the mean $\pm$ SD. The p-value was calculated using one-way ANOVA followed by the Tukey–Kramer multiple-comparison test. **$p < 0.005$. ns; not significant. (D, E) Hematoxylin and eosin staining (D) and magnetic resonance imaging (E) in mouse groups indicated above. Note that no tumors are seen in *Tip60* knockout mice. Images are representative, and white arrows indicate tumors. Scale bars: 200 μm.

from *EGFR^{TL}/CCSP-rtTA/Cre/Tip60$^{wt/wt}$* (II) or *EGFR^{TL}/CCSP-rtTA/Cre/Tip60$^{F/wt}$* (III) mice (Figure 4D). Magnetic resonance imaging analysis also revealed lung tumors in *EGFR^{TL}/CCSP-rtTA/Cre/Tip60$^{wt/wt}$* (II) and in *EGFR^{TL}/CCSP-rtTA/Cre/Tip60$^{F/wt}$* (III) mice, but no tumors were evident in *EGFR^{TL}/CCSP-rtTA/Cre/Tip60$^{F/F}$* (IV) mice (Figure 4E). These results indicate that TIP60 expression is required for lung tumorigenesis.

2.4 | Identification of candidate TIP60 targets by RNA-seq and ChIP-seq

Next, to identify TIP60 effectors, we performed RNA-seq and ChIP-seq in shTIP60-1, shTIP60-2, and control H1975 cells. Analysis for DEGs revealed a large number of both downregulated and upregulated genes in H1975-shTIP60 cells relative to control cells, with more genes being downregulated (Figure 5A,B). Furthermore, hierarchical clustering analysis of DEGs showed consistent expression changes in H1975-shTIP60-1 and shTIP60-2 relative to control cells (Figure 5C). TIP60 reportedly acetylates multiple lysine residues on histone H4[4]; thus we used an antipan-acetyl H4 antibody for ChIP-seq. As shown in Figure 5D and Figure S6A, we identified 13 overlapping genes whose expression and histone H4 acetylation signal were both reduced by TIP60 suppression. Among them, we first focused on TGM2, a member of the transglutaminase family, which is reportedly associated with tumor growth or patient poor prognosis in colorectal carcinoma, glioblastoma, and pancreatic cancer[17–19]; however, TGM2 knockdown had no effect on tumor growth in H1975 cells (data not shown). Thus we next focused on TGM5, which is also a member of the transglutaminase family. H4 acetylation levels at the *TGM5* gene significantly decreased in both H1975-shTIP60-1 and -2 cells relative to controls (Figure 5E), suggesting that *TGM5* is a target of TIP60.

We next examined TCGA database to investigate Kaplan–Meier survival analysis of lung adenocarcinoma patients. The median overall survival of the patients in the high TGM5 score group was significantly shorter than that of the patients in the low TGM5 group (Figure 5F).

We then assessed TGM5 expression after either silencing or overexpressing (OE) TIP60 in H1975 and A549 cells. TIP60 knockdown decreased TGM5 expression in both lines (Figure 5G; lanes 1 vs. 2; lanes 5 vs. 6). By contrast, TIP60 OE did not increase TGM5 expression in H1975 cells (Figure 5G; lanes 3 vs. 4) but did in A549 cells (Figure 5G; lanes 7 vs. 8). To determine whether TIP60 enzymatic activity was required for TGM5 regulation, constructs of wild-type

(WT) TIP60, TIP60-G380A (inactive mutation, mut), or an empty vector were transfected into TIP60 knockdown (KD) cells (H1975 shTIP60-2 under DOX treatment). TGM5 expression was upregulated in H1975 TIP60-KD cells transiently transfected with the WT TIP60 vector relative to those transfected with the mut TIP60 vector (Figure S3A). These results suggest that TGM5 is downstream of TIP60 in lung cancer cells. To further investigate TGM5 function in NSCLC cells, we silenced TGM5 expression by transfecting H1975 cells with pools of siRNAs specifically targeting TGM5 mRNA and then confirmed TGM5 downregulation at both mRNA and protein levels (Figure 5H,I). TGM5 knockdown significantly decreased cell growth (Figure 5J) and migration (Figure 5K,L) relative to control H1975 cells. Furthermore, to examine whether TGM5 overexpression compensates for TIP60 suppression, we repeated this analysis using H1975 TIP60-KD cells transiently transfected with a TGM5 or an empty vector. Immunoblot analysis confirmed continuous suppression of TIP60 with DOX treatment and TGM5 overexpression in H1975 TIP60-KD cells transiently transfected with the TGM5 vector relative to those transfected with the empty vector (Figure S6B). Migration and invasive activities were significantly increased by TGM5 overexpression relative to control cells (Figure S6D,E). In addition, TGM5 overexpression tended to increase the cell number of H1975 TIP60 KD cells relative to control cells (Figure S6C). These results suggest that TIP60 regulates lung tumor growth, at least in part via TGM5.

2.5 | Targeting TIP60 suppresses tumor progression in lung cancer

To identify compounds that might inhibit TIP60 expression, we used a connectivity map[20] and detected five high-scoring compounds (Figure 6A). We investigated TIP60 inhibiting efficacy among these compounds, and found that artemether inhibited TIP60 expression relative to other compounds in both H1975 and A549 cells (Figure S7A). Artemether is a derivative of artemisinin, which is a natural product derived from the Chinese herb *Artemisia annua* L. and widely used as an antimalarial drug.[21] Artemisinin downregulated TIP60 expression at lower concentrations than artemether in H1975 and A549 cells (Figure 6B and Figure S7B); thus we selected artemisinin for further experiments. Dose-dependent downregulation of TIP60 expression was observed in H1975 and A549 cells but less potent TIP60 downregulation in BEAS-2B cells (Figure 6B). Interestingly, BEAS-2B cells showed significantly a higher IC$_{50}$ for artemisinin than did H1975 or A549
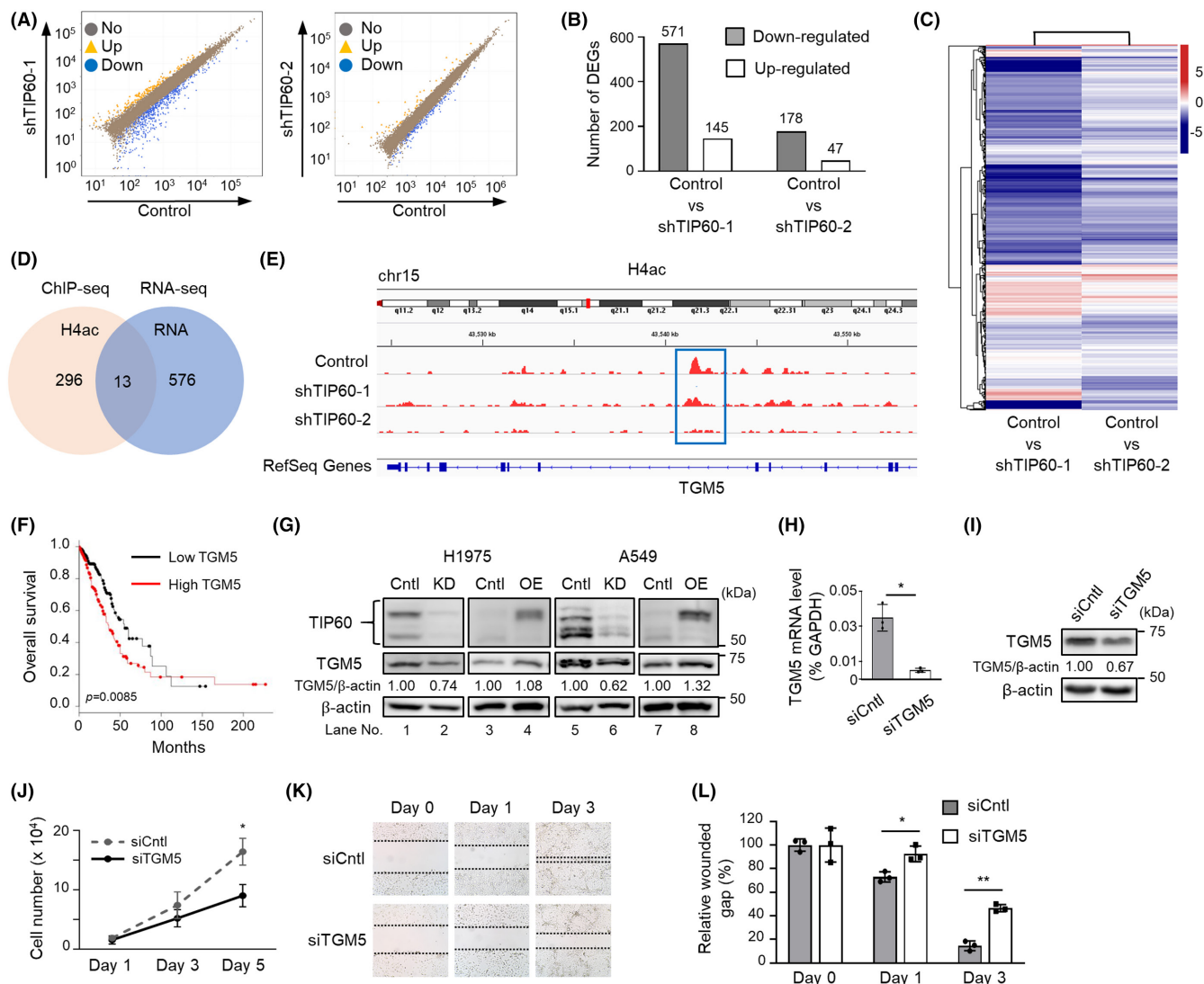
FIGURE 5 TGM5 is a candidate gene downstream of TIP60 and may contribute to tumor progression. (A, B) Scatter plots (A) and number of DEGs (B) showing that, relative to control cells, H1975-shTIP60-1, and shTIP60-2 cells exhibit a greater number of downregulated than upregulated genes. (C) Hierarchical clustering analysis of DEGs showing consistent expression changes in pairwise comparisons of H1975 shTIP60-1 and shTIP60-2 cells relative to control cells. (D) Venn diagram showing numbers of differential genes between ChIP-seq (pink circle) and RNA-seq (blue circle). In total, 13 genes were identified as overlapping. (E) ChIP-seq signals at the *TGM5* gene locus showing decreased enrichment for H4 acetylation in shTIP60-1 and shTIP60-2 relative to control cells (in a blue rectangle). (F) Kaplan–Meier survival analysis of lung adenocarcinoma showing poor prognosis of patients in the TGM5 high expression group. Data were extrapolated from TCGA. The *p*-value was determined using the log-rank test. (G) Immunoblot showing efficacy of siTIP60 knockdown or TIP60 overexpression and changes of TGM5 expression in H1975 and A549 cells. Cells were transiently transfected with TIP60 siRNA or control siRNA for 72 h and then immunoblotted. All blots show representative images, and analysis of TGM5/β-actin was calculated using ImageJ software. (H, I) qPCR (H) and immunoblot (I) showing efficacy of TGM5 knockdown by siRNA in H1975 cells. H1975 cells were transfected with siRNA pools specific for TGM5 mRNA or non-targeting control for 72 h, and then subjected to qPCR and immunoblot. qPCR data are the mean ± SD of triplicates from one experiment and are representative of three independent experiments. Blots show representative images, and analysis of TGM5/β-actin was calculated using ImageJ software. (J) Cell growth assay of H1975 TGM5 knockdown or control cells. (K, L) Wound healing assay showing suppressed migration of H1975 TGM5 knockdown compared with control cells. Wound gaps (day 0) were made after transfection with TGM5 siRNA. Images of wounded cell monolayers are representative of three independent experiments. Data relevant to relative wound gaps are the mean ± SD of triplicates from one experiment and are representative of three independent experiments. The *p*-value was calculated using the unpaired two-tailed Welch's *t*-test. *$p < 0.05$ and **$p < 0.005$.

cells (Figure 6C). Accordingly, the MTS assay revealed significant inhibition of H1975 and A549 cell viability by artemisinin treatment compared with those of BEAS-2B cells (Figure 6D). Furthermore, artemisinin treatment significantly inhibited cell growth, migration, and invasive activities relative to cells treated with DMSO in H1975 and A549 cells (Figure S7C–H). Next, to determine whether artemisinin treatment induces cell death by suppressing TIP60, we treated H1975-OE, A549-OE, or corresponding control cells
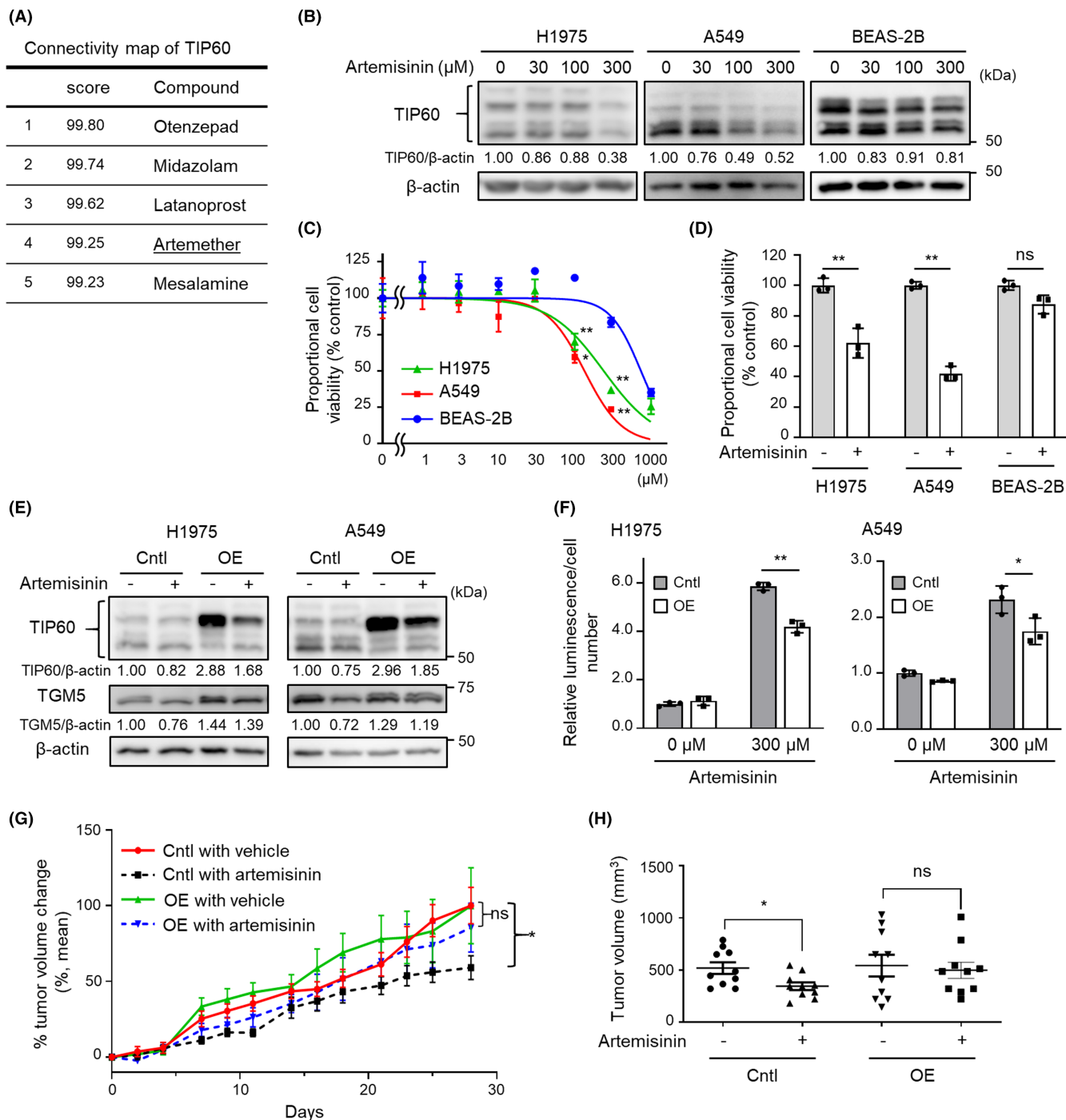
FIGURE 6 Artemisinin suppresses tumor progression by downregulating TIP60. (A) Connectivity map of TIP60 showing five compounds ranked by relative scores. (B) Immunoblot showing dose-dependent TIP60 downregulation by artemisinin treatment. At each concentration, cells were treated for 72 h with artemisinin before proteins were subjected to immunoblot. Blots show representative images, and analysis of TIP60/β-actin was calculated using ImageJ software. (C) Dose inhibition curves and SDs of artemisinin-treated H1975, A549, and BEAS-2B cells. (D) Viability assay showing that artemisinin treatment decreases cell viability. Cells were incubated for 72 h with artemisinin (300 μM) or DMSO (control) prior to determination of cell viability. (E) Immunoblot showing a change in TIP60 and TGM5 expression following artemisinin treatment of control (Cntl) or TIP60 overexpressing (OE) H1975 and A549 cells. Cells were treated 72 h with artemisinin (300 μM) and then immunoblotted. Blots show representative images, and analyses of TIP60/β-Actin and TGM5/β-actin were calculated using ImageJ software. (F) Changes in caspase-3/7 activity following artemisinin treatment of control or H1975 and A549-OE cells. Cells were incubated for 24 h with artemisinin (300 μM) prior to the analysis of caspase-3/7 activity, which was normalized to cell number. Data are the mean ± SD of triplicates from one experiment and are representative of two independent experiments. (G, H) Analysis of tumor volume change and tumor volume in mouse xenograft tumor models harboring control or A549-OE cells. Nude mice bearing A549 Cntl or A549-OE cells (10 tumors/5 mice per group) were treated with vehicle or artemisinin (200 mg/kg orally once daily) for 28 days. Mice were monitored for changes in tumor volume. Data are presented as the mean percentage change in tumor volume ± SEM. The p-value was calculated using the unpaired two-tailed Welch's t-test. *$p < 0.05$ and **$p < 0.005$. ns; not significant.

with artemisinin and assayed Caspase-3/7 activity as an apoptotic marker. Artemisinin treatment decreased TIP60 expression in both control and OE cells, although TGM5 expression was inhibited only in controls (Figure 6E). Caspase-3/7 activity was increased by artemisinin treatment in H1975 and A549 control cells (Figure 6F), while upregulation of Caspase-3/7 activity in response to artemisinin treatment seen in control cells was significantly attenuated in H1975-OE and A549-OE cells (Figure 6F). These results suggest that artemisinin treatment induces NSCLC cell apoptosis.

Next, we generated mouse xenograft models by injecting A549-TIP60 OE or control (Cntl) cells subcutaneously into nude mice. After tumors reached optimal volume (100–200 mm³), we administered artemisinin at 200 mg/kg or vehicle orally once daily for 4 weeks. Artemisinin treatment did not alter body weight in either mouse line (Figure S8A). However, artemisinin treatment significantly inhibited tumor growth in mice bearing A549-Cntl xenografts relative to vehicle-treated mice, whereas the antitumor efficacy of artemisinin treatment was less potent in mice implanted with A549-OE cells (Figure 6G,H).

To demonstrate that TIP60 acetyltransferase activity is required for tumorigenesis, we treated lung tumors with TH1834, a TIP60 acetyltransferase inhibitor,[22] in cell culture and in vivo. TH1834 treatment suppressed histone H4 acetylation and TGM5 expression in a dose-dependent manner in H1975 and A549 cells (Figure 7A). We next treated H1975 and A549 cells with TH1834 and observed a significant inhibition of cell growth, migration, and invasive activities in both cell lines (Figure 7B–F). Last, to investigate the effects of TH1834 in vivo, we used xenograft mouse models injected with A549 cells. After tumors reached optimal volume (100–200 mm³), we administered TH1834 at 10 mg/kg or vehicle intraperitoneally five times per week for 3 weeks.[23] Body weight remained unchanged by TH1834 treatment (Figure S8B). TH1834 treatment significantly inhibited tumor growth in mice bearing A549 tumors relative to vehicle-treated mice (Figure 7G,H). Taken together, these findings suggest that targeting TIP60 could have an antitumor effect in the context of lung cancer.

3 | DISCUSSION

In this study, we showed that TIP60 knockdown in an in vivo model of lung cancer inhibits lung tumor formation and progression. We also reveal that TGM5 is downstream of TIP60 and contributes to tumor progression in lung cancer. Furthermore, artemisinin or TH1834 treatment suppressed tumor growth in cell culture and in vivo, suggesting that targeting TIP60 might be a novel treatment for lung cancer (Figure 8).

By acetylating histone proteins, KAT enzymes transform closed chromatin into a more relaxed opened structure that enables the binding of various transcription factors. Depending on which histone protein residues are acetylated or what transcription factors bind to active chromatin sites, KATs either promote or suppress tumorigenesis. GCN5, a KAT family member, reportedly promotes tumor progression in several cancers,[24,25] although neither homozygous nor heterozygous GCN5 knockout inhibits tumorigenesis in transgenic tumor mice models (manuscript in preparation), possibly because GCN5 promotes tumor growth but does not inhibit apoptosis of lung cancer cells.[24] TIP60 has a sequence distinct from that of GCN5 and acetylates different histones,[26] suggesting that TIP60 rather than GCN5 is crucial for lung tumorigenesis. Here, we showed that TIP60 was expressed at low levels in multiple lung cancer lines and in clinical lung tumor tissues relative to expression seen in normal tissues, initially suggesting that TIP60 serves as a tumor suppressor. However, TIP60 overexpression neither inhibited tumor progression nor induced tumor cell apoptosis. In fact, TIP60 knockdown in H1975 and A549 cells inhibited cell growth, migration, and invasion activities, which is consistent with a previous report.[27] In contrast, another paper reported the antitumor activity of TIP60 using lung cancer cells.[28] This is possibly because different methods or conditions were used to generate knockdown or overexpression experiments. Although the role of TIP60 in lung cancer is controversial, we showed that homozygous Tip60 knockout in vivo suppressed tumor formation in the lung, strongly indicating that TIP60 is required for tumor formation and progression in the lung as a coactivator. Furthermore, our

FIGURE 7 TH1834 inhibits tumor progression by downregulating TIP60 enzymatic activity. (A) Immunoblot showing dose-dependent downregulation of acetylated histone H4 and TGM5 by TH1834 treatment. At each concentration, cells were treated for 48 h with TH1834 before proteins were subjected to immunoblot. Blots show representative images. (B) TH1834 treatment inhibits cell growth in H1975 or A549 cells. Cell numbers were determined on days 1, 3, and 5 after TH1834 (80 μM) or DMSO addition. Data are the mean ± SD of triplicates from one experiment and are representative of three independent experiments. (C, D) Wound healing assay showing suppressed migration of H1975 (C) or A549 (D) cells treated with TH1834 (80 μM) relative to those cells treated with DMSO. Images of wounded cell monolayers are representative of three independent experiments. Data relevant to relative wound gaps are the mean ± SD of triplicates from one experiment and are representative of three independent experiments. (E, F) Transwell invasion assay showing the significant difference in invasion activities between H1975 (E) or A549 (F) cells treated with TH1834 (80 μM) versus the corresponding cells treated with DMSO. Images of invasive cells are representative of three independent experiments. Data relevant to relative invasive cell number are the mean ± SD of three invasive cell number/field from one experiment and are representative of three independent experiments. (G, H) Analysis of tumor volume change (G) and tumor volume (H) in mouse xenograft tumor models harboring A549 cells. Nude mice bearing A549 cells (8–10 tumors/4 or 5 mice per group) were treated with vehicle or TH1834 (10 mg/kg intraperitoneally once daily five times a week) for 21 days. Mice were monitored for changes in tumor volume. Data are presented as the mean percentage change in tumor volume ± SEM. The p-value was calculated using the unpaired two-tailed Welch's t-test. *p < 0.05 and **p < 0.005. ns; not significant.
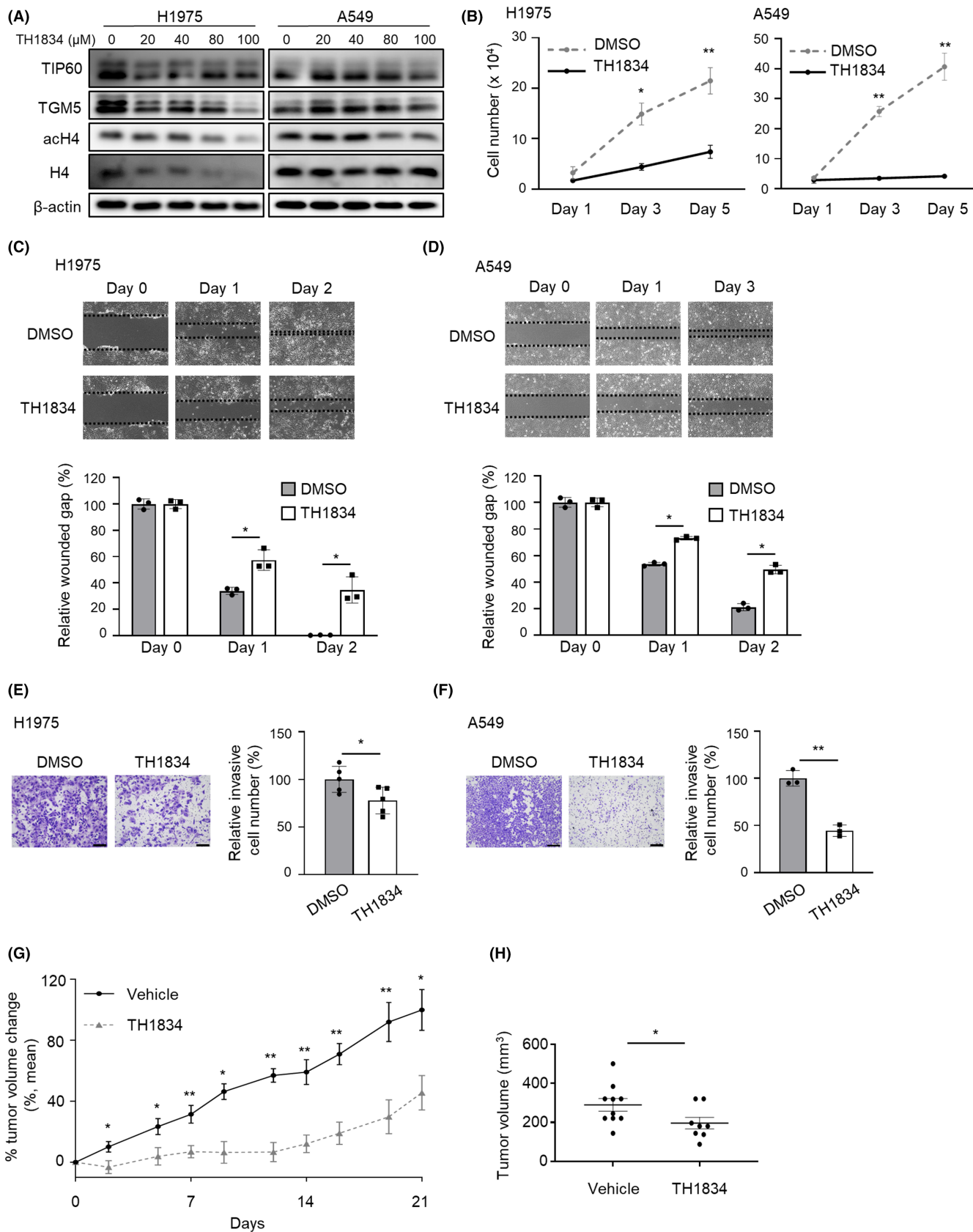
findings are consistent with previous studies suggesting that some cancer cells require low TIP60 levels for survival and the observation that eliminating already low TIP60 protein levels induces cancer cell death.[27,29] Interestingly, homozygous *Tip60* deletion

had no overt effect on normal lung tissues, although *Tip60* loss is lethal for embryogenesis and hematopoietic stem cell maintenance.[15,30] These results suggest that TIP60 function is context dependent and critical for lung cancer cells but not for normal lung

FIGURE 8 Model for the role of TIP60 in lung cancer.
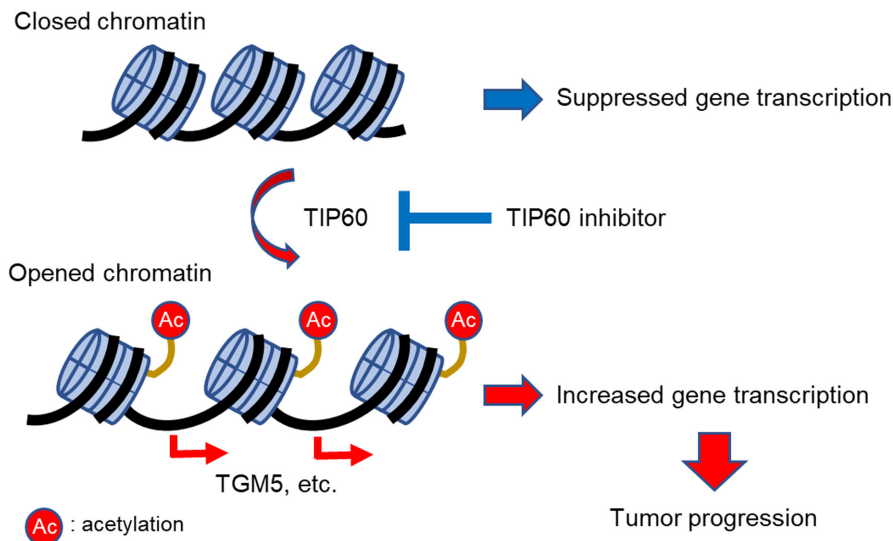
cells. Furthermore, despite evidence that TIP60 serves as a coactivator, TIP60 overexpression did not promote tumor progression. Assuming that the minimal expression required for TIP60 activity is set at a lower point in lung cancer and has already reached a plateau, TIP60 overexpression might have no effect on tumor progression. Indeed, 50% loss of TIP60 (via heterozygous knockout) still exceeded the threshold level for TIP60 activity, resulting in tumorigenesis, whereas loss of all TIP60 expression (via homozygous knockout) completely inhibited tumor formation in mouse lungs. It has been previously reported that reducing PU.1 expression to 20% but not 50% of normal levels promoted the development of acute myeloid leukemia,[31] indicating graded control of tumor formation by specific molecules. Of note, the relative difference in TIP60 expression levels between normal (higher) and tumor (lower) cells indicates that TIP60 suppression could have tumor-specific efficacy against lung cancer.

Our ChIP-seq and RNA-seq analyses revealed TGM5 to be downstream of TIP60, and a potential contributor to tumor progression and migration capacity. In addition, involucrin, which is cross-linked to membrane proteins by transglutaminase, and TGM2 are also among the 13 genes found to be downstream of TIP60, suggesting that transglutaminase plays specific roles in TIP60 regulatory activities. Transglutaminase family members are cross-linking enzymes that catalyze the formation of isopeptide bonds between the γ-carboxamide group of protein-bound glutamine and the ε-amino group of lysine residues,[32] and they function in cell adhesion, differentiation, and signal transduction.[33,34] However, TGM5 function in cancer remains unclear, whereas TGM2 is known to promote tumor cell differentiation, mobility, invasion, and survival.[33,35] Indeed we showed that TGM5 activity decreased tumor progression, at least in part. Intriguingly, TGM5 is reportedly acetylated,[36] suggesting that TIP60 may regulate TGM5 activity by directly acetylating TGM5. Furthermore, a polymorphism on chromosome 15q15.2, where *TGM5* is located,[37] is significantly associated with NSCLC,[38] further linking TGM5 with

NSCLC. Taken together, we conclude that TIP60 regulates tumor activities, at least in part through TGM5, which is likely to play a so far unknown role in lung cancer.

To efficiently inhibit TIP60, we used a connectivity map database and selected artemisinin. We report that artemisinin treatment inhibited TIP60 expression and tumor progression. TIP60 regulates transcription of various genes, including *NF-κB*, *MYC*, and *CCND1*,[39–41] all also blocked by artemisinin and associated with antitumor activities of artemisinin,[42–44] suggesting that artemisinin exerts multiple anticancer effects via TIP60 regulation. However, artemisinin is not an ideal and specific compound for clinical suppression of TIP60 in part because high concentrations are required to inhibit TIP60 expression. To improve its bioavailability and efficacy, several derivatives have been synthesized, among them dihydroartemisinin and artesunate. In early phase clinical trials, combination therapies, including artemisinin derivatives, with chemotherapy showed safety and high efficacy,[45,46] although the data were limited and larger scale phase clinical trials are needed. Artemisinin may also have antitumor activity independent of TIP60 inhibition. Accordingly, we utilized TH1834, a TIP60 acetyltransferase inhibitor, to treat lung tumors in cell culture and *in vivo*. Tumor growth was suppressed, although a high concentration was still required for treatment. Therefore, a novel drug that specifically targets TIP60 is urgently needed. Recently, the degradation of targeted proteins using PROTACs has emerged as a promising therapeutic modality. PROTACs consist of three parts—a ligand of the protein of interest (POI), a ligand of an E3 ubiquitin ligase, and a linker—induce ubiquitylation and subsequent proteasomal degradation of the POI.[47] As PROTACs can target epigenetic proteins[48] or undruggable targets such as DNA-binding proteins (e.g., transcription factors),[49] the generation of a PROTAC targeting TIP60 could be an attractive approach to lung cancer treatment.

In summary, we show here that TIP60 is required for the malignant transformation of pulmonary epithelial cells. Understanding this mechanism is significant, as it could lead to novel and much-needed therapy for lung cancer.

DATA AVAILABILITY STATEMENT

The RNA-seq and ChIP-seq data are available from the NCBI GEO database (GSE207202 and GSE207201). All other data are available in the main text or the supplementary materials.

ETHICS STATEMENT

Approval of the research protocol by an Institutional Reviewer Board: N/A. Informed Consent: N/A. Registry and the Registration No. of the study/trial: N/A. Animal Studies: All animal studies were approved by the Institutional Animal Care and Use Committee at Beth Israel Deaconess Medical Center (#094–2020).

ORCID

Susumu S. Kobayashi https://orcid.org/0000-0003-2262-4001

REFERENCES

1. Siegel RL, Miller KD, Fuchs HE, Jemal A. Cancer statistics, 2021. *CA Cancer J Clin*. 2021;71:7-33.
2. Verdone L, Agricola E, Caserta M, Di Mauro E. Histone acetylation in gene regulation. *Brief Funct Genomic Proteomic*. 2006;5:209-221.
3. Sapountzi V, Logan IR, Robson CN. Cellular functions of TIP60. *Int J Biochem Cell Biol*. 2006;38:1496-1509.
4. Squatrito M, Gorrini C, Amati B. Tip60 in DNA damage response and growth control: many tricks in one HAT. *Trends Cell Biol*. 2006;16:433-442.
5. Tang Y, Luo J, Zhang W, Gu W. Tip60-dependent acetylation of p53 modulates the decision between cell-cycle arrest and apoptosis. *Mol Cell*. 2006;24:827-839.
6. Charvet C, Wissler M, Brauns-Schubert P, et al. Phosphorylation of Tip60 by GSK-3 determines the induction of PUMA and apoptosis by p53. *Mol Cell*. 2011;42:584-596.
7. Fang X, Lu G, Ha K, et al. Acetylation of TIP60 at K104 is essential for metabolic stress-induced apoptosis in cells of hepatocellular cancer. *Exp Cell Res*. 2018;362:279-286.
8. Kim JH, Kim B, Cai L, et al. Transcriptional regulation of a metastasis suppressor gene by Tip60 and beta-catenin complexes. *Nature*. 2005;434:921-926.
9. Gorrini C, Squatrito M, Luise C, et al. Tip60 is a haplo-insufficient tumour suppressor required for an oncogene-induced DNA damage response. *Nature*. 2007;448:1063-1067.
10. Mattera L, Escaffit F, Pillaire MJ, et al. The p400/Tip60 ratio is critical for colorectal cancer cell proliferation through DNA damage response pathways. *Oncogene*. 2009;28:1506-1517.
11. Bassi C, Li YT, Khu K, et al. The acetyltransferase Tip60 contributes to mammary tumorigenesis by modulating DNA repair. *Cell Death Differ*. 2016;23:1198-1208.
12. Ikura T, Ogryzko VV, Grigoriev M, et al. Involvement of the TIP60 histone acetylase complex in DNA repair and apoptosis. *Cell*. 2000;102:463-473.
13. Edmond V, Moysan E, Khochbin S, et al. Acetylation and phosphorylation of SRSF2 control cell fate decision in response to cisplatin. *EMBO J*. 2011;30:510-523.
14. Fisher JB, Horst A, Wan T, Kim MS, Auchampach J, Lough J. Depletion of Tip60 from In vivo Cardiomyocytes increases myocyte density, followed by cardiac dysfunction, myocyte fallout and lethality. *PLoS One*. 2016;11:e0164855.
15. Numata A, Kwok HS, Zhou QL, et al. Lysine acetyltransferase Tip60 is required for hematopoietic stem cell maintenance. *Blood*. 2020;136:1735-1747.
16. Li D, Shimamura T, Ji H, et al. Bronchial and peripheral murine lung carcinomas induced by T790M-L858R mutant EGFR respond to HKI-272 and rapamycin combination therapy. *Cancer Cell*. 2007;12:81-93.
17. Malkomes P, Lunger I, Oppermann E, et al. Transglutaminase 2 promotes tumorigenicity of colon cancer cells by inactivation of the tumor suppressor p53. *Oncogene*. 2021;40:4352-4367.
18. Yin J, Oh YT, Kim JY, et al. Transglutaminase 2 inhibition reverses mesenchymal Transdifferentiation of glioma stem cells by regulating C/EBPbeta signaling. *Cancer Res*. 2017;77:4973-4984.
19. Wang F, Wang L, Qu C, et al. Kaempferol induces ROS-dependent apoptosis in pancreatic cancer cells via TGM2-mediated Akt/mTOR signaling. *BMC Cancer*. 2021;21:396.
20. Subramanian A, Narayan R, Corsello SM, et al. A next generation connectivity map: L1000 platform and the first 1,000,000 profiles. *Cell*. 2017;171(1437–1452):e1417.
21. Eastman RT, Fidock DA. Artemisinin-based combination therapies: a vital tool in efforts to eliminate malaria. *Nat Rev Microbiol*. 2009;7:864-874.
22. Gao C, Bourke E, Scobie M, et al. Rational design and validation of a Tip60 histone acetyltransferase inhibitor. *Sci Rep*. 2014;4:5372.
23. Wang X, Wan TC, Kulik KR, et al. Pharmacological inhibition of the acetyltransferase Tip60 mitigates myocardial infarction injury. *Dis Model Mech*. 2023;16:dmm049786.
24. Chen L, Wei T, Si X, et al. Lysine acetyltransferase GCN5 potentiates the growth of non-small cell lung cancer via promotion of E2F1, cyclin D1, and cyclin E1 expression. *J Biol Chem*. 2013;288:14510-14521.
25. Farria AT, Plummer JB, Salinger AP, et al. Transcriptional activation of MYC-induced genes by GCN5 promotes B-cell lymphomagenesis. *Cancer Res*. 2020;80:5543-5553.

26. Sheikh BN, Akhtar A. The many lives of KATs - detectors, integrators and modulators of the cellular environment. *Nat Rev Genet*. 2019;20:7-23.

27. Liang Z, Yu Q, Ji H, Tian D. Tip60-siRNA regulates ABCE1 acetylation to suppress lung cancer growth via activation of the apoptotic signaling pathway. *Exp Ther Med*. 2019;17:3195-3202.

28. Yang Y, Sun J, Chen T, et al. Tat-interactive protein-60KDA (TIP60) regulates the tumorigenesis of lung cancer In vitro. *J Cancer*. 2017;8:2277-2281.

29. Brown JA, Bourke E, Eriksson LA, Kerin MJ. Targeting cancer using KAT inhibitors to mimic lethal knockouts. *Biochem Soc Trans*. 2016;44:979-986.

30. Hu Y, Fisher JB, Koprowski S, McAllister D, Kim MS, Lough J. Homozygous disruption of the Tip60 gene causes early embryonic lethality. *Dev Dyn*. 2009;238:2912-2921.

31. Rosenbauer F, Wagner K, Kutok JL, et al. Acute myeloid leukemia induced by graded reduction of a lineage-specific transcription factor, PU.1. *Nat Genet*. 2004;36:624-630.

32. Candi E, Oddi S, Terrinoni A, et al. Transglutaminase 5 cross-links loricrin, involucrin, and small proline-rich proteins in vitro. *J Biol Chem*. 2001;276:35014-35023.

33. Lorand L, Graham RM. Transglutaminases: crosslinking enzymes with pleiotropic functions. *Nat Rev Mol Cell Biol*. 2003;4:140-156.

34. Kárpáti S, Sárdy M, Németh K, et al. Transglutaminases in autoimmune and inherited skin diseases: the phenomena of epitope spreading and functional compensation. *Exp Dermatol*. 2018;27:807-814.

35. Huang L, Xu AM, Liu W. Transglutaminase 2 in cancer. *Am J Cancer Res*. 2015;5:2756-2776.

36. Rufini A, Vilbois F, Paradisi A, et al. Transglutaminase 5 is acetylated at the N-terminal end. *Amino Acids*. 2004;26:425-430.

37. Grenard P, Bates MK, Aeschlimann D. Evolution of transglutaminase genes: identification of a transglutaminase gene cluster on human chromosome 15q15. Structure of the gene encoding transglutaminase X and a novel gene family member, transglutaminase Z. *J Biol Chem*. 2001;276:33066-33078.

38. Rafnar T, Sulem P, Besenbacher S, et al. Genome-wide significant association between a sequence variant at 15q15.2 and lung cancer risk. *Cancer Res*. 2011;71:1356-1361.

39. Kim JW, Jang SM, Kim CH, An JH, Kang EJ, Choi KH. New molecular bridge between RelA/p65 and NF-kappaB target genes via histone acetyltransferase TIP60 cofactor. *J Biol Chem*. 2012;287:7780-7791.

40. Liu R, Gou D, Xiang J, et al. O-GlcNAc modified-TIP60/KAT5 is required for PCK1 deficiency-induced HCC metastasis. *Oncogene*. 2021;40:6707-6719.

41. Dalvai M, Bellucci L, Fleury L, Lavigne AC, Moutahir F, Bystricky K. H2A.Z-dependent crosstalk between enhancer and promoter regulates cyclin D1 expression. *Oncogene*. 2013;32:4243-4251.

42. Efferth T. From ancient herb to modern drug: Artemisia annua and artemisinin for cancer therapy. *Semin Cancer Biol*. 2017;46:65-83.

43. Li J, Feng W, Lu H, et al. Artemisinin inhibits breast cancer-induced osteolysis by inhibiting osteoclast formation and breast cancer cell proliferation. *J Cell Physiol*. 2019;234:12663-12675.

44. Wang T, Wang J, Ren W, Liu ZL, Cheng YF, Zhang XM. Combination treatment with artemisinin and oxaliplatin inhibits tumorigenesis in esophageal cancer EC109 cell through Wnt/beta-catenin signaling pathway. *Thorac Cancer*. 2020;11:2316-2324.

45. von Hagens C, Walter-Sack I, Goeckenjan M, et al. Prospective open uncontrolled phase I study to define a well-tolerated dose of oral artesunate as add-on therapy in patients with metastatic breast cancer (ARTIC M33/2). *Breast Cancer Res Treat*. 2017;164:359-369.

46. Deeken JF, Wang H, Hartley M, et al. A phase I study of intravenous artesunate in patients with advanced solid tumor malignancies. *Cancer Chemother Pharmacol*. 2018;81:587-596.

47. Bekes M, Langley DR, Crews CM. PROTAC targeted protein degraders: the past is prologue. *Nat Rev Drug Discov*. 2022;21:181-200.

48. Bassi ZI, Fillmore MC, Miah AH, et al. Modulating PCAF/GCN5 immune cell function through a PROTAC approach. *ACS Chem Biol*. 2018;13:2862-2867.

49. Bai L, Zhou H, Xu R, et al. A potent and selective small-molecule degrader of STAT3 achieves complete tumor regression *in vivo*. *Cancer Cell*. 2019;36(5):498-511.

SUPPORTING INFORMATION

Additional supporting information can be found online in the Supporting Information section at the end of this article.